"Bad Urban" Uplink Multipaths' Distribution in Azimuth-Elevation DOA, with Scatterers Modeled as Inside a Cylinder Above the Mobile & as More Sparse with Height

Andriy Yakovych OLENKO (olenk@univ.kiev.ua)
Dept. of Probability Theory & Mathematical Statistics, Kyiv University, Kyiv, 01033, Ukraine

Sajjad Ahmed QASMI
Sandvine Incorporated, Waterloo, Ontario, N2L 3V3, Canada

Kainam Thomas WONG (ktwong@ieee.org)
Department of Electronic & Information Engineering,
Hong Kong Polytechnic University, Hung Hom, Kowloon, Hong Kong

***Abstract*— This paper presents a new bivariate joint distributions of uplink multipaths' two-dimensional (2D) azimuth-elevation direction-of-arrival (DOA) for a landmobile cellular wireless communication system. These distributions are based on a "geometrical" model of the three-dimensional (3D) spatial relationships among the mobile-station (MS), the scatterers, and the base-station (BS). This "geometric model" has the scatterers spatially distributed inside an above-ground 3D vertical cylinder whose flat bottom circular base centers at the mobile, and whose density tapers off as height increases. These distributions are rigorously derived via thorough mathematics, and expressed in closed form explicitly in terms of the DOA variables.**

I. Introduction

The present work will *rigorously derive* the uplink received-signals' multipaths' arrival delays and two-dimensional arrival angles from an idealized geometry assuming all scatterers to be spatially distributed non-uniformly in a vertical column of uniform circular cross-section with its base on the x-y plane centered around the mobile, and with its density tapering off towards zero as height increases.

Within the geometric-modeling literature that analytically derives closed-form explicit expressions for a radiowave communication fading channel's multipath TOA and/or AOA distributions (please refer to the literature survey in [2]), almost all earlier references:

1) model the scatterers' spatial distribution as only two-dimensionally horizontal, thereby ignoring the elevation dimension and restricting the DOA to azimuth only, or
2) focus on marginal probability density functions of either the TOA or the azimuth-only AOA, versus trivariate and bivariate probability density functions of the TOA and the 2D-AOA as in this work.

The key exceptions are [1], [2], and [3]. In [1], a closed-form explicit expression is derived analytically for the downlink azimuth-elevation AOA bivariate probability density function and for the uplink azimuth-AOA univariate marginal probability density function, assuming the scatterers as uniformly distributed inside a "semi-spheroid" (i.e., a sliced top from a sphere); however, no consideration is given to the TOA. In [2], the scatterers' spatial density is modeled instead as over an hemisphere centered around the mobile, then closed-form explicit expressions are derived analytically of the TOA-DOA's trivariate, bivariate and univariate distributions for the uplink and the downlink. [3] instead models the scatterers as cylindrically distributed around the mobile to mimic high-rises in "bad urban" propagation settings, with the scatterers' spatial density uniform within that finite-height cylinder. The present work will allow this spatial density to taper off to zero as height increases, to better mimic physical reality.

II. A New Cylindrical Model with $f_z(z) \to 0$ as $z \to \infty$

Referring to Figure 1, a cellular basestation, located at the Cartesian coordinates $(x, y, z) = (0, 0, 0)$, communicates with a mobile transmitter located in the Cartesian coordinates $(x, y, z) = (D, 0, 0)$. The mobile's transmitted signal bounces off exactly one scatterer before reaching the basestation receiver. A multipath's time-of-arrival τ and the azimuth-elevation direction-of-arrival are determined by the spatial location of the scatterer off which the multipath is reflected. Subsequent mathematical analysis will use both sets of spherical coordinates defined in Figure 1: the coordinates (r, ϕ, θ) are centered at the base-station, whereas the coordinates (r_M, ϕ_M, θ_M) are centered at the mobile.

[0]The first author was supported by the Swedish Institute grant SI-01424/2007. The third author was supported by the Internal Competitive Research Grant number G.42.R6.YF52 from the Hong Kong Polytechnic University.

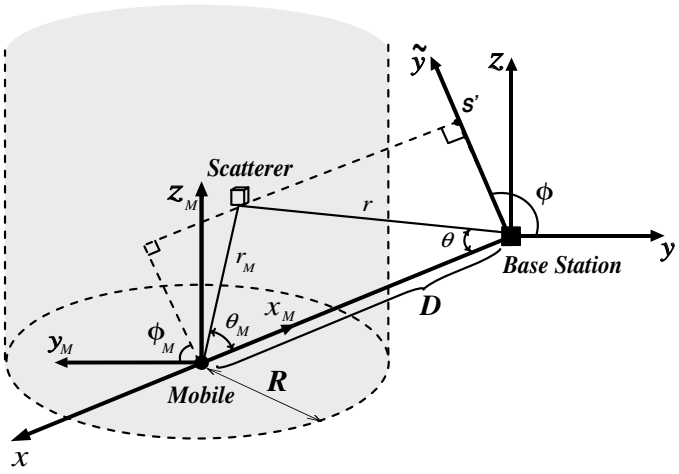

Fig. 1. The uplink/downlink Cartesian/spherical coordinates relating the mobile, an arbitrary scatterer, and the base-station.

A. The Scatterers' Spatial Distribution & Characteristics

Like all earlier papers (please refer to the literature survey in [2]) that analytically derive closed-form explicit expressions of the AOA-TOA distributions based on geometrical models, these standard assumptions are made:

1) Each propagation path, between the mobile and the base-station, reflects off exactly one scatterer.
2) Each scatterer acts as an isotropic lossless re-transmitter, independently of other scatterers.
3) Complex-phase effects in the receiving-antenna's vector-summation of the arriving-multipaths may be overlooked. That is, all arriving multipaths arriving at each receiving-antenna are assumed to be temporally in-phase among themselves.
4) All antennas are isotropic, at both the base-station and the mobile.
5) Polarizational effects may be overlooked.

Assume the scatterers to be distributed within an above-ground cylinder with a flat base of radius $R \leq D$ centered around the mobile. A cylindrical model has been investigated in [3], where the scatterers' spatial density is uniform within the cylinder. That is, $f_z(z)$ is a positive constant. More physically realistic than that uniform density is this following "strongly positive function" model allowing the scatter density to $gradually$ taper off to zero as height increases:

$$f_z(z) \quad = \quad \begin{cases} \frac{2}{3H}, & \text{if } z \in [0, H] \\ \frac{2H^2}{3z^3}, & \text{if } z > H \end{cases} \tag{1}$$

which does not vanish for $z > H$ but becomes increasingly sparse as z increases beyond. This nonuniform scatterer density means that fewer multipaths arrive at the basestation from higher up from the ground level. This is intuitively appealing because a higher elevation DOA (with reference to the base-station) generally necessitates a longer sequence of zigzag reflections from the mobile transmitter up along the high-rises. These reflections incur power loss, which could be modeled by having the higher-altitude scatterers having less re-transmission power or as having fewer single-bounce scatterers higher up from the ground level. The above spatial-distribution's azimuth-symmetry around the mobile means no azimuth direction is "favored" or "disfavored".

III. Uplink Trivariate Joint Density of the TOA & the Azimuth-Elevation DOA

The following tries to relate a scatterer's Cartesian spatial location at (x, y, z) to the corresponding TOA τ and the two-dimensional DOA (ϕ, θ). First, convert from the Cartesian coordinates (x, y, z) to the spherical coordinates (r, ϕ, θ) of Figure 1, $f_{r,\phi,\theta}(r, \phi, \theta)$

$$\begin{aligned} &= \left. \frac{f_{x,y,z}(x, y, z)}{|J_1(x, y, z)|} \right|_{x=r\cos(\theta), y=r\sin(\theta)\cos(\phi), z=r\sin(\theta)\sin(\phi)} \\ &= r^2 \sin(\theta) f_{x,y,z}\left(r\cos(\theta), r\sin(\theta)\cos(\phi), r\sin(\theta)\sin(\phi)\right) \end{aligned} \tag{2}$$

with the Jacobian,

$$\begin{aligned} &J_1(x, y, z)|_{x=r\cos(\theta), y=r\sin(\theta)\cos(\phi), z=r\sin(\theta)\sin(\phi)} \\ &= \left| \begin{array}{ccc} \frac{\partial x}{\partial r} & \frac{\partial x}{\partial \phi} & \frac{\partial x}{\partial \theta} \\ \frac{\partial y}{\partial r} & \frac{\partial y}{\partial \phi} & \frac{\partial y}{\partial \theta} \\ \frac{\partial z}{\partial r} & \frac{\partial z}{\partial \phi} & \frac{\partial z}{\partial \theta} \end{array} \right|^{-1} = -\left[r^2 \sin(\theta)\right]^{-1} \end{aligned}$$

Next, convert from the spherical coordinates (r, ϕ, θ) to the TOA-DOA coordinates (τ, ϕ, θ) [1]. The propagation-path's total delay equals:

$$\tau \quad = \quad \frac{r + r_M}{c} \quad = \quad \frac{D}{c}\left[\frac{r}{D} + \sqrt{1 + \left(\frac{r}{D}\right)^2 - 2\frac{r}{D}\cos(\theta)}\right] \tag{3}$$

Hence,

$$\begin{aligned} J_2\left(r, \phi, \theta\right)|_{r=s_0} \quad &= \quad \left|\frac{dr}{d\tau}\right|_{r=s_0}^{-1} \\ &= \quad \frac{2}{c}\frac{\left[\cos(\theta) - \left(\frac{\tau c}{D}\right)\right]^2}{\left[1 + \left(\frac{\tau c}{D}\right)^2 - 2\frac{\tau c}{D}\cos(\theta)\right]} \quad \stackrel{\text{def}}{=} \quad \frac{1}{A_\tau} \end{aligned}$$

where $s_0 = \frac{D}{2}\frac{1-\left(\frac{\tau c}{D}\right)^2}{\cos(\theta) - \frac{\tau c}{D}}$ due to (3). All scatterers that have $z \leq H$ would satisfy

$$s_0 \sin(\theta)\sin(\phi) \quad \leq \quad H. \tag{4}$$

The inequality $y^2 + (x - D)^2 \leq R^2$ is equivalent to $\left(\frac{s_0}{D}\right)^2 \sin^2(\theta)\cos^2(\phi) + \left(\frac{s_0}{D}\cos(\theta) - 1\right)^2 \leq \left(\frac{R}{D}\right)^2$, which in turn is equivalent to

$$\begin{aligned} \widetilde{\mathcal{B}} \quad &= \quad \frac{\left[\left(\frac{\tau c}{D}\right)^2 - 1\right]\cos(\theta)}{\frac{\tau c}{D} - \cos(\theta)} \\ &\quad - \frac{\left[\left(\frac{\tau c}{D}\right)^2 - 1\right]^2}{4\left[\frac{\tau c}{D} - \cos(\theta)\right]^2}\left(\sin^2(\theta)\cos^2(\phi) + \cos^2(\theta)\right) \\ &\geq \quad 1 - \left(\frac{R}{D}\right)^2 \end{aligned}$$

[1] Figure 1's spherical coordinates are designed to render the Jacobian $J_2\left(r, \phi, \theta\right)$ independent of ϕ.

The above steps give the trivariate joint distribution, of the uplink multipaths' TOA and azimuth-elevation DOA:

$$\begin{aligned} & f_{\tau,\phi,\theta}(\tau,\phi,\theta) \\ = & \left.\frac{f_{r,\phi,\theta}(r,\phi,\theta)}{|J_2(r,\phi,\theta)|}\right|_{r=s_0} \\ = & \left. A_\tau r^2 \sin\theta f_{x,y,z}\left(r\cos\theta, r\sin(\theta)\cos(\phi), r\sin(\theta)\sin(\phi)\right)\right|_{r=s_0} \\ = & \begin{cases} A_\tau \frac{\sin\theta}{\pi}\left(\frac{s_0}{R}\right)^2 f_z(s_0\sin\theta\sin\phi), & \text{if } \phi\in[0,\pi], \widetilde{\mathcal{B}} \geq 1-\left(\frac{R}{D}\right)^2 \\ 0, & \text{otherwise} \end{cases} \end{aligned}$$

Substituting in (1), the above formula becomes:

$$\begin{aligned} & f_{\tau,\phi,\theta}(\tau,\phi,\theta) \\ = & \begin{cases} 0, & \text{if } \phi\notin[0,\pi] \\ & \text{or } \widetilde{\mathcal{B}} < 1-\left(\frac{R}{D}\right)^2 \\ \frac{2}{3}\left(\frac{s_0}{R}\right)^2 \frac{A_\tau}{H}\frac{\sin(\theta)}{\pi}, & \text{else if } s_0\sin(\theta)\sin(\phi)\leq H \\ & \text{and } \phi\in[0,\pi] \\ & \text{and } \widetilde{\mathcal{B}} \geq 1-\left(\frac{R}{D}\right)^2 \\ \frac{2}{3}\left(\frac{H}{R}\right)^2 \frac{A_\tau}{s_0}\frac{1}{\pi\sin^2(\theta)\sin^3(\phi)}, & \text{if } s_0\sin\theta\sin\phi > H \\ & \text{and } \phi\in[0,\pi] \\ & \text{and } \widetilde{\mathcal{B}} \geq 1-\left(\frac{R}{D}\right)^2 \end{cases} \end{aligned}$$

IV. Uplink Bivariate Joint Density of ϕ and θ

Towards deriving $f_{\phi,\theta}(\phi,\theta)$, this section needs to mathematically characterize the intersection of the constant-(ϕ,θ) line with the cylinder of scatterers. As the constant-(ϕ,θ) line radiates outwards from the origin, this line will first touch the cylinder at its lateral surface. This first contact point corresponds to the shortest propagation-delay $\tau_{\min}$. On the other hand, constant-(ϕ,θ) line's last contact with the cylinder is on the cylinder's lateral surface. Between these two points, the constant (ϕ,θ) line would intersect the $z=H$ plane. Due to (1), in this case there are changes in the density.

The following will identify the support-range of θ at a specific $\phi\in[0,\pi]$. Referring to Figure 2, consider a point A, lying either on (i) the cylinder's lateral surface, or (ii) the $z=H$ plane. Point A projects onto the horizontal Cartesian $x-y$ plane (i.e., the ground) at point C. For the distance between the point B (i.e., the base-station) and point C,

$$|BC|^2 = [r\cos(\theta)]^2 + [r\sin(\theta)\cos(\phi)]^2. \quad (5)$$

For both cases (i) and (ii), the first contact must be on the cylinder's lateral surface, giving $|CM|=R$. For fixed ϕ, the upper limit for θ is obtained at $\angle BCM=\frac{\pi}{2}$. Thus, $\frac{R}{D} = \frac{|CK|}{|BC|} = \frac{r}{|BC|}\sin(\theta)\cos(\phi)$. With (5), $\left[\frac{D}{R}\sin(\theta)\cos(\phi)\right]^2 = \cos^2(\theta)+\sin^2(\theta)\cos^2(\phi)$. This implies that the upper limit for the θ support-region, for any $\phi\in[0,\pi]$, equals $\arctan(\bar{a}_\theta)$, where $\bar{a}_\theta = \frac{1}{|\cos(\phi)|\sqrt{\left(\frac{D}{R}\right)^2-1}}$.

Next, the analysis will identify the range of τ over which to integrate $f_{\tau,\phi,\theta}(\tau,\phi,\theta)$ to produce $f_{\phi,\theta}(\phi,\theta)$, for a particular (ϕ,θ). From (3),

$$\frac{\partial\tau}{\partial r} = \frac{1}{c}\left(1+\frac{\frac{r}{D}-\cos(\theta)}{\sqrt{\left(\frac{r}{D}\right)^2-2\left(\frac{r}{D}\right)\cos(\theta)+1}}\right) \geq 0 \quad (6)$$

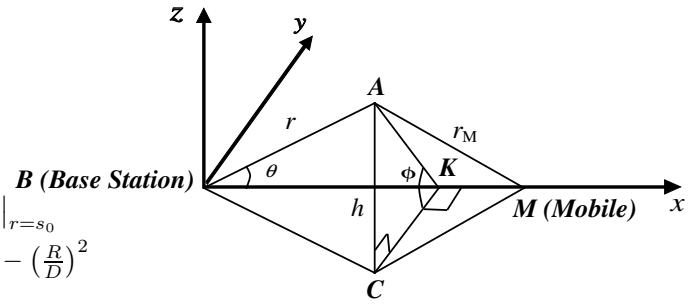

Fig. 2. This figure aids the identification of the range of θ at a specific $\phi\in[0,\pi]$ such that $f_{\phi,\theta}(\phi,\theta)\neq 0$. The point A lies on either (i) the cylinder's lateral surface, or (ii) the $z=H$ plane. For either case, point A projects onto the horizontal Cartesian x-y plane (i.e., the ground) at point C; and the distance $|CM|$ between the Point C and the mobile must not exceed R.

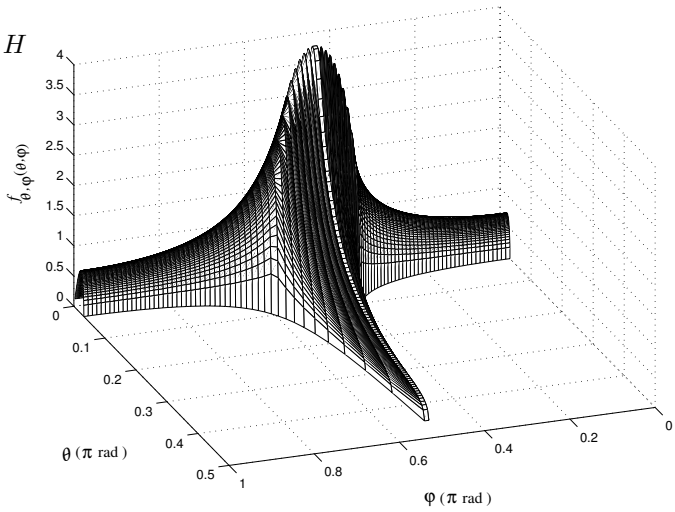

Fig. 3. The uplink bivariate 2D-AOA distribution for scattering around the mobile in form of cylindrical narrowing cross section with D = 1000m, R = 100m and H = 300m

The non-negativity implies τ to be non-decreasing as r increases.

For case (i), $|CM|=R$. Given (6), the extrema of the above-mentioned range of τ are located at where the cylinder's lateral surface $y^2+(x-D)^2=R^2$ intersects with the (ϕ,θ) line. Figure 2 imposes the constraint $\left(\frac{R}{D}\right)^2 = \left[1-\frac{r}{D}\cos(\theta)\right]^2 + \left[\frac{r}{D}\sin(\theta)\cos(\phi)\right]^2$. The latter implies that $r_{\max}, r_{\min} = D\left[\frac{\cos(\theta)\pm\sqrt{\left(\frac{R}{D}\right)^2[1-\sin^2(\theta)\sin^2(\phi)]-\sin^2(\theta)\cos^2(\phi)}}{1-\sin^2(\theta)\sin^2(\phi)}\right]$. By definition, $\tau = \frac{r+r_M}{c}$, but Figure 2 gives $r_M = \sqrt{R^2+[r\sin(\theta)\sin(\phi)]^2}$. Hence,

$$\tau_{\max} = \frac{1}{c}\left[r_{\max}+\sqrt{R^2+\left(r_{\max}\sin(\theta)\sin(\phi)\right]^2}\right) \quad (7)$$

$$\tau_{\min} = \frac{1}{c}\left[r_{\min}+\sqrt{R^2+\left(r_{\min}\sin(\theta)\sin(\phi)\right]^2}\right) \quad (8)$$

For case (ii), the constant-(ϕ,θ) line crosses the $z=H$ plane for a second time at point A. At this point A, $|CM| \leq R$ and $z=H$. Hence, $r = \frac{H}{\sin(\phi)\sin(\theta)}$,

$$r_M \;=\; \sqrt{r^2+D^2-2rD\cos(\theta)} \;=\; D\sqrt{\left[\frac{H}{D}\frac{1}{\sin(\phi)\sin(\theta)}\right]^2 - 2\frac{H}{D}\frac{\cot(\theta)}{\sin(\phi)}+1}.$$

Hence,

$$\tilde{\tau} = \frac{r+r_M}{c} = \frac{D}{c}\left\{\frac{H}{D}\frac{1}{\sin(\phi)\sin(\theta)} + \sqrt{\left[\frac{H}{D}\frac{1}{\sin(\phi)\sin(\theta)}\right]^2 - 2\frac{H}{D}\frac{\cot(\theta)}{\sin(\phi)}+1}\right\}.$$

The $\tau_{\min}$ of (8), derived under case (i), still holds for case (ii). This is because, $\tau_{\min}$ must correspond to the first intersection with the cylinder as the constant-(ϕ,θ) line radiates outwards from the origin. This first intersection must occur on the cylinder's lateral surface.

Only if the constant-(ϕ,θ) line intersects with the cylinder of scatterers, will $f_{\phi,\theta}(\phi,\theta) \neq 0$. The support-region $\{(\phi,\theta)|f_{\phi,\theta}(\phi,\theta)\neq 0\}$ is $\phi\in[0,\pi]$ and $\theta\in[0,\bar{a}_\theta]$.

Integration with respect to τ gives:

$$f_{\phi,\theta}(\phi,\theta) \;=\; \begin{cases} \int_{\tau_{\min}}^{\tau_{\max}} A_\tau \frac{\sin\theta}{\pi}\left(\frac{s_0}{R}\right)^2 f_z\left(s_0\sin(\theta)\sin(\phi)\right)d\tau, & \text{if } \phi\in[0,\pi],\ \theta\in[0,\arctan(\bar{a}_\theta)] \\ 0, & \text{otherwise} \end{cases} \tag{9}$$

As it was mentioned above, there are two cases: one $z>H$ and another for $z<H$. $\tilde{\tau}$ which corresponds to $z=H$ is derived above. The general formula (9) becomes:

$$f_{\phi,\theta}(\phi,\theta) \;=\; \begin{cases} 0, & \text{if } \phi\notin(0,\pi) \\ & \text{or } \theta\notin(0,\arctan(\bar{a}_\theta)] \\ \frac{2}{3}\frac{\sin\theta}{\pi}\int_{\tau_{\min}}^{\tau_{\max}}\left(\frac{s_0}{R}\right)^2\frac{A_\tau}{H}\,d\tau & \\ = \frac{2}{3}\,F(\tau_{\min},\tau_{\max}), & \text{if } \tilde{\tau}\geq\tau_{\max} \\ & \text{and } \phi\in(0,\pi) \\ & \text{and } \theta\in(0,\arctan(\bar{a}_\theta)] \\ \frac{2}{3}\left(\frac{H}{R}\right)^2\frac{1}{\pi\sin^2\theta\sin^3\phi}\int_{\tau_{\min}}^{\tau_{\max}}\frac{A_\tau}{s_0}\,d\tau & \text{if } \tilde{\tau}\leq\tau_{\min} \\ = \frac{2}{3}\left(\frac{H}{R}\right)^2\frac{1}{\pi\sin^2\theta\sin^3\phi}\,K(\tau_{min},\tau_{max}), & \text{and } \phi\in(0,\pi) \\ & \text{and } \theta\in(0,\arctan(\bar{a}_\theta)] \\ \frac{2}{3}\frac{\sin\theta}{\pi}\int_{\tau_{\min}}^{\tilde{\tau}}\left(\frac{s_0}{R}\right)^2\frac{A_\tau}{H}\,d\tau & \\ +\frac{2}{3}\left(\frac{H}{R}\right)^2\frac{1}{\pi\sin^2\theta\sin^3\phi}\int_{\tilde{\tau}}^{\tau_{\max}}\frac{A_\tau}{s_0}\,d\tau & \text{if } \tau_{\min}<\tilde{\tau}<\tau_{\max} \\ = \frac{2}{3}\,F(\tau_{\min},\tilde{\tau}) + \frac{2}{3}\left(\frac{H}{R}\right)^2\frac{1}{\pi\sin^2\theta\sin^3\phi}\,K(\tilde{\tau},\tau_{\max}), & \text{and } \phi\in(0,\pi) \\ & \text{and } \theta\in(0,\arctan(\bar{a}_\theta)] \end{cases} \tag{10}$$

where $K(\tau_1,\tau_2)=\int_{\tau_1}^{\tau_2}\frac{A_\tau}{s_0}d\tau = \ln\left(\frac{\left[1-\left(\frac{\tau_2 c}{D}\right)^2\right]\left[\left(\cos\theta-\frac{\tau_1 c}{D}\right)\right]}{\left[1-\left(\frac{\tau_1 c}{D}\right)^2\right]\left[\cos\theta-\left(\frac{\tau_2 c}{D}\right)\right]}\right)$, and $F(\tau_1,\tau_2)=\int_{\tau_1}^{\tau_2}\frac{A_\tau\sin(\theta)}{H\pi}\left(\frac{s_0}{R}\right)^2 d\tau = (c(6D^8\tau_1+4c^2\tau_1^3-6D^8\tau_2+18c^2D^6\tau_1^2\tau_2-18c^4D^4\tau_1^4\tau_2+6c^6D^2\tau_1^6\tau_2-18c^2D^6\tau_1\tau_2^2-12c^4D^4\tau_1^3\tau_2^2-4c^2D^6\tau_2^3+12c^4D^4\tau_1^2\tau_2^3-12c^6D^2\tau_1^4\tau_2^3+4c^8\tau_1^6\tau_2^3+18c^4D^4\tau_1\tau_2^4+12c^6D^2\tau_1^3\tau_2^4-6c^6D^2\tau_1\tau_2^6-4c^8\tau_1^3\tau_2^6-3cD(\tau_1^2-\tau_2^2)(7D^6-3c^2D^4(\tau_1^2+\tau_2^2)+4c^6\tau_1^2\tau_2^2(\tau_1^2+\tau_2^2)+c^4D^2(\tau_1^4-11\tau_1^2\tau_2^2+\tau_2^4))\cos\theta+6D^2(D^6(\tau_1-\tau_2)+3c^2D^4\tau_1(\tau_1-\tau_2)\tau_2+3c^4D^2\tau_1\tau_2(\tau_2^3-\tau_1^3)+c^6\tau_1\tau_2(\tau_1^5-\tau_2^5))\cos 2\theta-3cD^7\tau_1^2\cos 3\theta+3c^3D^5\tau_1^4\cos 3\theta-c^5D^3\tau_1^6\cos 3\theta+3cD^7\tau_2^2\cos 3\theta-3c^3D^5\tau_2^4\cos 3\theta+c^5D^3\tau_2^6\cos 3\theta)\sin\theta)/(144H\pi R^2(-c\tau_1+D\cos\theta)^3(c\tau_2-D\cos\theta)^3)$,

REFERENCES

[1] R. Janaswamy, "Angle of Arrival Statistics for a 3D Spheroid Model," *IEEE Transactions on Vehicular Technology*, vol. 51, no. 5, pp. 1242-1247, September 2002.

[2] A. Y. Olenko, K. T. Wong, S. A. Qasmi & J. Ahmadi-Shokouh, "Analytically Derived Uplink/Downlink TOA & 2D-DOA Distributions with Scatterers in a 3D Hemispheroid Surrounding the Mobile," *IEEE Transactions on Antennas & Propagation*, vol. 54, no. 9, pp. 2446-2454, September 2006.

[3] A. Y. Olenko, K. T. Wong & S. A. Qasmi "Distribution of 'Bad Urban' Uplink Multipaths' Arrival Delay & Azimuth-Elevation Arrival Angles, with Scatterers Cylindrically Distributed Above the Mobile," *IEEE Global Telecommunications Conference*, SPC04-4, 2006.